

## Construction and structure studies of DNA-bipyridine complexes as versatile scaffolds for site-specific incorporation of metal ions into DNA

Rui Wang, Srivathsan V. Ranganathan, Phensinee Haruehanroengra, Song Mao, Matteo Scalabrin, Daniele Fabris, Alan Chen, Hehua Liu, Abdalla E.A. Hassan, Jianhua Gan & Jia Sheng

To cite this article: Rui Wang, Srivathsan V. Ranganathan, Phensinee Haruehanroengra, Song Mao, Matteo Scalabrin, Daniele Fabris, Alan Chen, Hehua Liu, Abdalla E.A. Hassan, Jianhua Gan & Jia Sheng (2018): Construction and structure studies of DNA-bipyridine complexes as versatile scaffolds for site-specific incorporation of metal ions into DNA, Journal of Biomolecular Structure and Dynamics, DOI: [10.1080/07391102.2018.1441071](https://doi.org/10.1080/07391102.2018.1441071)

To link to this article: <https://doi.org/10.1080/07391102.2018.1441071>

 View supplementary material [↗](#)

 Accepted author version posted online: 15 Feb 2018.  
Published online: 22 Feb 2018.

 Submit your article to this journal [↗](#)

 Article views: 29

 View related articles [↗](#)

 View Crossmark data [↗](#)



## Construction and structure studies of DNA-bipyridine complexes as versatile scaffolds for site-specific incorporation of metal ions into DNA

Rui Wang<sup>a,b</sup>, Srivathsan V. Ranganathan<sup>b</sup>, Phensinee Haruehanroengra<sup>a,b</sup>, Song Mao<sup>a,b</sup>, Matteo Scalabrin<sup>a,b</sup>, Daniele Fabris<sup>a,b</sup>, Alan Chen<sup>a,b</sup>, Hehua Liu<sup>c</sup>, Abdalla E.A. Hassan<sup>d</sup>, Jianhua Gan<sup>c\*</sup> and Jia Sheng<sup>a,b\*</sup>

<sup>a</sup>Department of Chemistry, University at Albany, State University of New York, 1400 Washington Ave., Albany, NY 12222, USA;

<sup>b</sup>The RNA Institute, University at Albany, State University of New York, 1400 Washington Ave., Albany, NY 12222, USA; <sup>c</sup>State Key Laboratory of Genetic Engineering, Collaborative Innovation Center of Genetics and Development, Department of Physiology and Biophysics, School of Life Sciences, Fudan University, Shanghai 200433, China; <sup>d</sup>Applied Nucleic Acids Research Center, Faculty of Science, Zagazig University, Zagazig, Egypt

Communicated by Ramaswamy H. Sarma

(Received 6 November 2017; accepted 12 February 2018)

The facile construction of metal–DNA complexes using ‘Click’ reactions is reported here. A series of 2'-propargyl-modified DNA oligonucleotides were initially synthesized as structure scaffolds and were then modified through ‘Click’ reaction to incorporate a bipyridine ligand equipped with an azido group. These metal chelating ligands can be placed in the DNA context in site-specific fashion to provide versatile templates for binding various metal ions, which are exchangeable using a simple EDTA washing-and-filtration step. The constructed metal–DNA complexes were found to be thermally stable. Their structures were explored by solving a crystal structure of a propargyl-modified DNA duplex and installing the bipyridine ligands by molecular modeling and simulation. These metal–DNA complexes could have wide applications as novel organometallic catalysts, artificial ribonucleases, and potential metal delivery systems.

**Keywords:** metallic DNA; click reaction; propargyl-DNA; DNA material; DNA scaffold

### 1. Introduction

DNA, the fundamental biomolecule of life, has increasingly emerged over the past few decades as a key building block and structural framework creating a myriad of functional materials (Cutler, Auyeung, & Mirkin, 2012; Macfarlane, O'Brien, Petrosko, & Mirkin, 2013; Rothmund, 2006; Seeman, 1982, 2010). These DNA-based materials are very attractive in both fundamental research and practical applications. For instance, owing to the unique base pairing specificity, predictability, and versatile programmability, DNA self-assembly has become an important strategy for the construction of nano-materials such as carbon nanotubes, nanobricks, metal nanoparticles, and quantum dots, etc. through a bottom-up method with precise design and control (Deng, Samanta, Nangreave, Yan, & Liu, 2012; Douglas, Dietz, et al., 2009; Douglas, Marblestone, et al., 2009; Kuzyk et al., 2012; Maune et al., 2010). In addition, the electrostatic properties and electrical conductivity of DNA as a highly charged polymer makes it attractive nanowire to fabricate nanoscale electro devices (Fink & Schönenberger, 1999; Klotsa, Römer, & Turner, 2005; Liu, Diao, & Nishi, 2008; Roche, 2003). More importantly, DNA is biodegradable and biocompatible, and therefore can work

as an excellent biofunctional framework for developing cell imaging probes, biocatalysts, drug deliver systems, and therapeutics (Chen, Groves, Muscat, & Seelig, 2015; Garg, Rath, & Goyal, 2015; Garg, Singh, Arora, & Murthy, 2012; Gupta, Tiwari, & Vyas, 2012; Wang, Huang, Yang, He, & Liu, 2013; Xu et al., 2014). These functional DNA molecules can be further used to construct small molecule–DNA hybrids that will largely increase the scope and versatility of their functional applications (Hong et al., 2015; McLaughlin, Hamblin, & Sleiman, 2011; Thaner, Eryazici, Farha, Mirkin, & Nguyen, 2014). It is well known that single-stranded DNA/RNA molecules, so-called aptamers, can be selected through SELEX technology (Systematic Evolution of Ligands by EXponential enrichment) (Ellington & Szostak, 1990; Robertson & Joyce, 1990; Tuerk & Gold, 1990) to bind almost every bimolecular target including proteins, carbohydrates, lipids, nucleic acids, and whole cells with extraordinarily high binding specificity and affinity. These DNA aptamers can serve as good structure scaffolds for the site-specific incorporation of diverse functionalities into any desired positions of the binding targets. In this sense, the hybrid complex of DNA-small molecules represents a general strategy to

\*Corresponding authors. Email: [ganjhh@fudan.edu.cn](mailto:ganjhh@fudan.edu.cn) (Jianhua Gan); [jsheng@albany.edu](mailto:jsheng@albany.edu) (Jia Sheng)

diversify the DNA building blocks and holds great promising to construct novel DNA based functional materials. However, although this DNA hybrid strategy has gained increasing popularity in nanostructure constructions, its applications in other areas, such as biocatalysis and organic synthesis, are yet to be explored probably due to the lack of feasible synthetic methods and the detailed structure information about small molecule–DNA interactions.

An interesting application that we are currently exploring involves constructing metallic DNA molecules as novel artificial ribonucleases to cleave target pathogenic RNA sequences, and as chiral catalysts to facilitate stereoselective organic transformations (Gjonaj & Roelfes, 2013; Oltra & Roelfes, 2008; Park et al., 2014; Sakamoto et al., 2003). These two functions can be achieved by the site-specific incorporation of metal ions into specific positions of DNA scaffolds that serve as either RNA targeting reagents (Hall, Husken, & Haner, 1996; Sakamoto et al., 2003; Williams et al., 2015) or chiral environments (Bos & Roelfes, 2014; Rioz-Martínez & Roelfes, 2015). Several methods have been developed for the site-specific introduction of metal ions into nucleic acids mainly through nucleobase–metal chelating or ‘click’ chemistry, a widely used bioorthogonal strategy to label macromolecules (Dey & Jäschke, 2015; Duprey, Takezawa, & Shionoya, 2013; Gierlich, Burley, Gramlich, Hammond, & Carell, 2006; Richters, Krug, Kösters, Hepp, & Müller, 2014; Scharf & Müller, 2013; Stubinitzky et al., 2014; Takezawa & Shionoya, 2012). However, the construction of a general scaffold or template that can bind a variety of metal ions for different functional applications has not been fully explored. In this paper, we demonstrated that the ‘click’ conjugation could be used to build this type of general platform for metal binding in a site-specific way. We first synthesized a series of DNA strands with previously reported 2'-propargyl modified nucleotide building blocks at different positions (1, Scheme 1), which can be subsequently linked to a metal chelating bipyridine ligand with a preinstalled azido group (2, Scheme 1) to make DNA–ligand–metal complexes (3, Scheme 1). These site-specifically located bipyridines can work as versatile platforms to bind different metal ions that are easily exchangeable using an EDTA-washing-and-filtration step (4, Scheme 1). In addition, the 3D structure information of this type of DNA–metal complex was also elucidated by X-ray crystallography and molecular simulation studies.

## 2. Results and discussion

### 2.1. Synthesis of metallic DNA through ‘Click’ reaction

Based on the synthetic feasibility of installing a reactive group into flexible locations of DNA, we chose the 2'-propargyl modified ribonucleotides as ideal DNA

building blocks, which are well compatible with solid phase synthesis and post-synthetic treatments. The minor-groove located propargyl groups have been demonstrated to produce modest perturbation of DNA biophysical properties such as duplex stability; and have been used to generate several fluorescent DNA probes (Berndl et al., 2009; Holzhauser, Rubner, & Wagenknecht, 2013; Yamada et al., 2011). For proof of principle, we synthesized a few single- and double-stranded DNA oligos containing each of the four 2'-propargyl (2'-prop)-A, C, G, and U in different sequence contexts. The modified products were purified by reverse phase HPLC and characterized by electrospray ionization mass spectrometry (ESI-MS, Table 1).

The selection of the metal binding ligands fell on a typical bipyridine structure, which has been previously applied to construct DNA-based asymmetric catalysts and functional nano-materials (Heck, Dumarcay, & Marsura, 2002; Ipe, Yoosaf, & Thomas, 2006), as the starting material to install the ‘Click’ active azido tags. As shown in Scheme 2, the treatment of 5,5'-dimethyl-bipyridine with *N*-bromosuccinimide (NBS) and azobisisobutyronitrile (AIBN) in a heated CCl<sub>4</sub> solution for 17 h produced a clean mixture of mono- and di-brominated bipyridine compounds with ~1:1 ratio, which can be separated by column chromatography. The mono-brominated product 6 was subsequently transferred to the azido-bipyridine 2 through the substitution of bromine by azide in a heated DMF solution with quantitative yield.

With these building blocks in hand, we carried out the ‘Click’ reaction using the standard CuBr catalyst in the presence of acetonitrile as Cu<sup>+</sup> chelating reagent. Although only moderate synthesis yields could be achieved for this Click conjugation, the products were easily separated from the substrates by our reverse phase HPLC conditions (see Section 4 for conditions). Exemplified in Figure 1, the incorporation of bipyridine ligand into DNA oligonucleotides decreased their retention time by about 2 min in our chromatogram, which suggested that these bipyridine–DNA complexes possessed a

Table 1. 2'-Propargyl modified DNA oligonucleotides.

| Entry | DNA sequence                     | MS (Calcd.)       |
|-------|----------------------------------|-------------------|
| 1     | CCAA(2'-prop-A)<br>GGTTACAGGTAAG | 5610.64 (5610.72) |
| 2     | CCAAAGGTTACA(2'-prop-G)<br>GTAAG | 5610.64 (5610.72) |
| 3     | TCGGGT(2'-prop-A)CCCGA           | 3700.67 (3700.45) |
| 4     | TCGGGTAC(2'-prop-C)CGA           | 3700.67 (3700.45) |
| 5     | TCG(2'-prop-G)GTACCCGA           | 3700.67 (3700.45) |
| 6     | TCGGG(2'-prop-U)ACCCGA           | 3686.38 (3686.45) |
| 7     | CGCGAAT(2'-prop-U)CGCG           | 3686.39 (3686.45) |
| 8     | G(2'-OMe-U)GTA(2'-prop-C)AC      | 2479.47 (2479.64) |
| 9     | G(2'-OMe-U)GT(2'-prop-A)CAC      | 2479.47 (2479.64) |

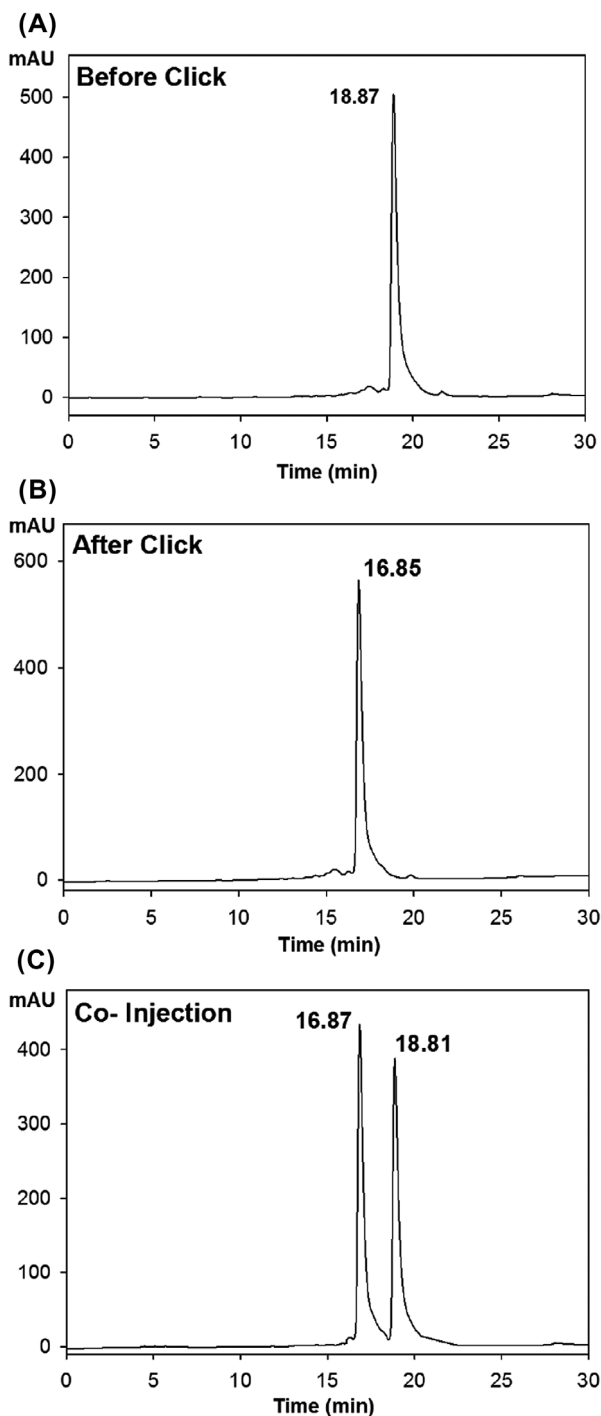


Figure 1. Analytical HPLC chromatograms obtained from 2'-propargyl-DNA 1 [5'-CCAA(2'-prop-A)GGTTACAGGTAAG] before (A) and after (B) 'Click' reaction with the bipyridine ligand. Panel (C) is the chromatogram obtained from the co-injected samples.

slightly higher overall polarity than the initial propargyl modified species. The separated substrate could be reused for the next cycle of 'Click' reaction.

Interestingly, the ESI-MS data clearly showed the presence of copper ion in the complex (Table 2, entry 1) after both reaction and purification, which can be explained by the strong binding of copper ion to the bipyridine ligand. The copper ion was subsequently washed out using 10 equivalents of EDTA through an ultrafiltration device with a 3 K-cut-off membrane. The concentrated solution was subsequently washed with water to obtain a metal-free species that could serve as a general template for the binding of other metal ions including  $\text{Cu}^{2+}$ ,  $\text{Ni}^{2+}$ ,  $\text{Zn}^{2+}$ , and  $\text{Cd}^{2+}$ . The corresponding metal-DNA complexes were shown to be very stable under the conditions employed for ESI-MS analysis (Table 2 and Figures S1–7). In order to further test their chemical stability, the metal-DNA oligonucleotide complexes were heated in 10 mM phosphate buffer (pH 7) under 60°C for 24 h and monitored by HPLC for possible strand cleavage. As exemplified in Figure S8 for DNA6- $\text{Cu}^{2+}$ , the metallic DNA oligonucleotides were thermally stable. These data demonstrated that bipyridine-directed chelation represents a general and versatile strategy to achieve site-specific incorporation of metal ions into different sites of DNA structure.

## 2.2. Thermal denaturation studies of metallic DNA duplexes

It has been shown that the propargyl modifications at the 2'-positions of DNA strand could increase the duplex stability when the DNA strand is hybridized with complementary RNA, whereas it can slightly destabilize the duplex when hybridized with DNA (Grøtli, Douglas, Eritja, & Sproat, 1998; Pujari, Leonard, & Seela, 2014). Consistent with these observations, as exemplified using DNA 2 in Table 1, the 2'-propargyl modified DNA duplex provided nearly the same  $T_m$  as the unmodified native species (black and blue curves in Figure 2), whereas the overall thermal stability decreased by 6.6°C for the duplex containing the additional bipyridine ligand (red curve in Figure 2), indicating certain extent of structural perturbation.

Table 2. Molecular Masses of DNA Oligonucleotide [5'-TCGGG(2'-prop-U)ACCCGA-3'] after 'Click' reaction and EDTA-aided ions exchange. The analysis was performed by ESI-MS as described in the experimental section.

| Entry | Metal Ions       | Calcd MS | Found MS |
|-------|------------------|----------|----------|
| 1     | After Click      | 3986.47  | 3986.67  |
| 2     | After Wash       | 3925.54  | 3925.75  |
| 3     | $\text{Cu}^{2+}$ | 3986.47  | 3986.66  |
| 4     | $\text{Cd}^{2+}$ | 4036.14  | 4036.64  |
| 5     | $\text{Zn}^{2+}$ | 3987.48  | 3987.67  |
| 6     | $\text{Ni}^{2+}$ | 3981.48  | 3981.67  |

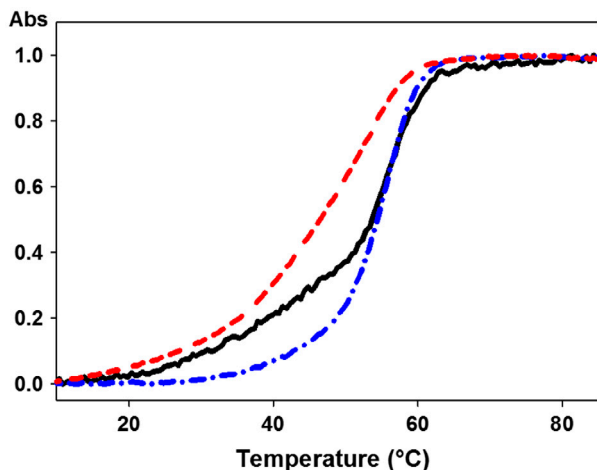


Figure 2. UV-melting temperature studies of native, 2'-propargyl modified, and dipyrindine 'Clicked' DNA duplexes. Sequences: DNA-2 in Table 1, 5'-CCAAAGGTTACAXG-TAAG-3', where X represents native dG (black), 2'-prop-G (blue) and 2'-dipyrindine-G (red), respectively, pairs with their native complementary strand 5'-CTTACCTGTAACCTTGG-3'. Their  $T_m$  values are 55.4, 55.1, and 48.8°C, respectively.

### 2.3. Crystal structure studies of 2'-propargyl modified DNA duplex

In order to explore the possible effects of these propargyl and bipyridine modifications on the DNA duplex structure, we successfully crystallized and solved a high-resolution structure of the self-complementary octamer duplex containing two 2'-propargyl-A residues (DNA-9 in Table 1) [5'-G(2'-OMe-dU)GT(2'-prop-A)CAC-3']<sub>2</sub>. In this construction, the 2'-OMe-dU residue was used to facilitate crystallization and drive the DNA sequence to fold into an A-form duplex without major structural perturbation, in analogy with the 2'-SeMe-dU functionality (Jiang, Sheng, Carrasco, & Huang, 2007; Sheng, Jiang, Salon, & Huang, 2007). This modified DNA oligonucleotide could crystallize under several different conditions of Nucleic Acid Mini-Screening and Natrix buffer kit within a few days. The crystals with best diffraction were grown under buffer conditions containing 10% 2-methyl-2,4-pentanediol (MPD), 40 mM sodium cacodylate (pH 7.0), 12 mM spermine tetra-HCl, 40 mM LiCl, 80 mM strontium chloride, and 20 mM magnesium chloride. The best crystal diffracted to 1.6 Å and the data collection/structure refinement statistics are summarized in Table 3.

The overall duplex structure and local 2'-prop-A:U pairing pattern are shown in Figure 3. Overall, there is no major structural perturbation caused by these two propargyl groups by comparing the modified DNA duplex with its native counterpart (Figure 3(A) and (B)), although the backbone of 2'-propargyl-A residue is

rotated for ~100 degree as observed in the base pairing pattern (Figure 3(C)). The 2'-propargyl groups were located in the minor groove of the duplex and turned to the 3'-direction of each strand. This arrangement leaves plenty of space for further modifications of the propargyl group within the minor groove.

### 2.4. Molecular simulation studies of metallic DNA duplex

The next step aimed at the characterization of the complete bipyridine conjugates to elucidate how the metal chelating ligands aligned in the DNA duplex. Unfortunately, all crystals obtained under many different conditions showed very weak and disordered diffraction patterns. This outcome suggested that, although the ligand might not affect the overall duplex structure, it was likely to adversely affect the molecular packing. As a possible alternative, we employed computational modeling to generate structures, in which two bipyridine ligands containing two copper ions were attached to the propargyl groups in the initial crystal structure. The final model of the whole complex was energy minimized and then subjected to molecular dynamic simulations. The comparison between the duplexes with and without the ligands revealed that the ligands did not significantly disrupt the helical structure of the duplex during the course of the simulation (see Supplementary Figure S9). However, it was interesting to note that the ligands adopted two distinct types of orientations as shown in Figure 4. The dominant configuration (~40%) adopted by the modified duplex involves one of the ligands reaching across the minor groove to form a salt bridge between the chelated copper ion and the phosphate group of two nucleotides to the 3' side of the complementary strand (Figure 4(A) and (C)). This across-the-groove binding by one of the ligands restricts the ability of the other ligand to simultaneously form another salt bridge, and hence is accommodated in the minor groove with the copper ion facing outward and solvated. The second configuration (~30%) involves both ligands simultaneously bound to phosphate groups, which are two nucleotides to the 3' side of their respective strands (Figure 4(B) and (D)). While this configuration allows for simultaneous formation of two salt bridges, we speculate that the entropic penalty associated with this state makes it less favorable than the single salt bridge state of the duplex, which also possesses a twofold symmetry due to the symmetrical nature of the duplex. Even though we observed both the symmetrical states of the dominant configuration, we did not observe a transition between the two due to the large energy barrier between the states. We surmise that the multiple orientations adopted by the ligands might have resulted in the poor resolution of their positions in the crystal structure.

Table 3. X-ray data collection and structural refinement statistics of 2'-propargyl modified DNA 8mer duplex [5'-G(2'-OMe-dU)GT(2'-prop-A)CAC-3']<sub>2</sub>.

|                                    | DNA-9 (PDB ID: 5E36)         |
|------------------------------------|------------------------------|
| <i>Data collection</i>             |                              |
| Space group                        | C222 <sub>1</sub>            |
| Unit cell (Å, °)                   | 32.0, 55.5, 75.7, 90, 90, 90 |
| Resolution range/last shell (Å)    | 30–1.6 (1.66–1.60)           |
| Unique reflections                 | 9231                         |
| Completeness (%)                   | 98.9                         |
| $R_{\text{merge}}$ (%)             | 7.2                          |
| $\langle I/\sigma(I) \rangle$      | 30.9                         |
| Redundancy                         | 5.7                          |
| <i>Refinement</i>                  |                              |
| Molecules per asymmetric unit      | 3 single strands             |
| Resolution range (Å)               | 27.76–1.60                   |
| Number of reflections              | 8752                         |
| Completeness (%)                   | 98.61                        |
| $R_{\text{work}}$ (%)              | 13.7                         |
| $R_{\text{free}}$ (%)              | 16.1                         |
| Bond length r.m.s. (Å)             | 0.048                        |
| Bond angle r.m.s.                  | 1.398                        |
| Overall B-factor (Å <sup>2</sup> ) | 10.87                        |

Note:  $R_{\text{merge}} = \sum |I - \langle I \rangle| / \sum I$ .

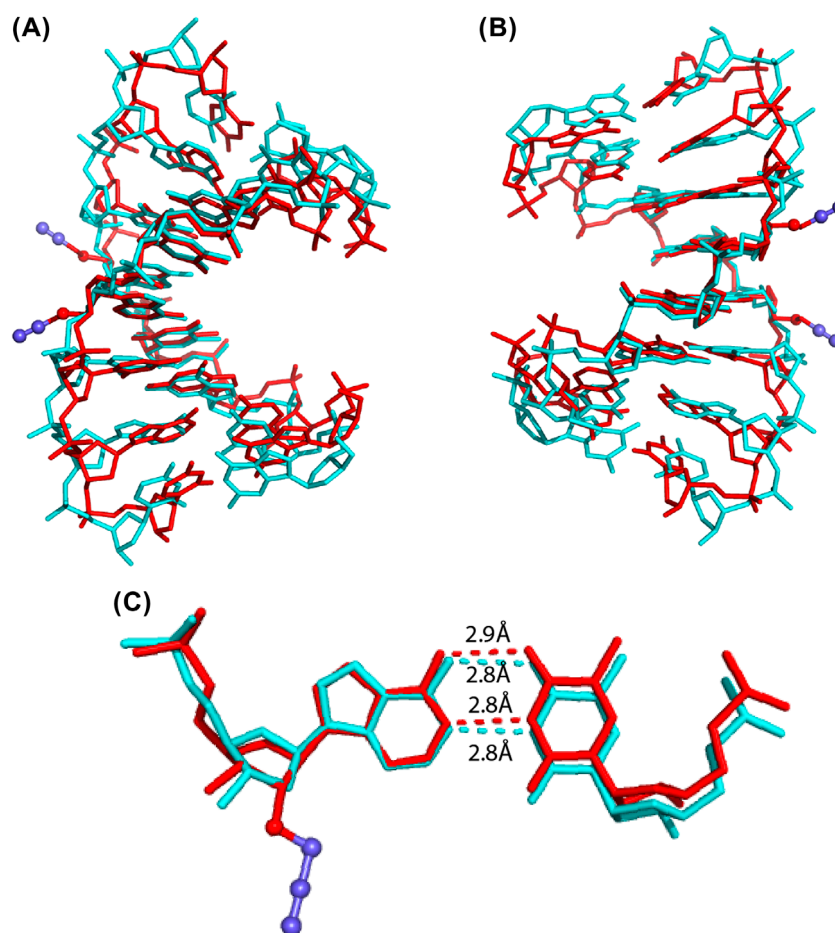


Figure 3. Structural features of octamer DNA duplex [5'-G(2'-OMe-dU)GT(2'-prop-A)CAC-3']<sub>2</sub>. (A) and (B) 180° rotation views of duplex superimposed comparison between propargyl modified 8mer (red) and native 8mer (cyan) (PDB ID: 1DNS), with the two 2'-propargyl groups stick into minor grooves. The observed r. m. s. d is 1.38 Å. (C) Base pair comparison of propargyl-A:T (red) and native A:T (cyan). The oxygen and carbon atoms are showed as red and blue spheres, respectively.

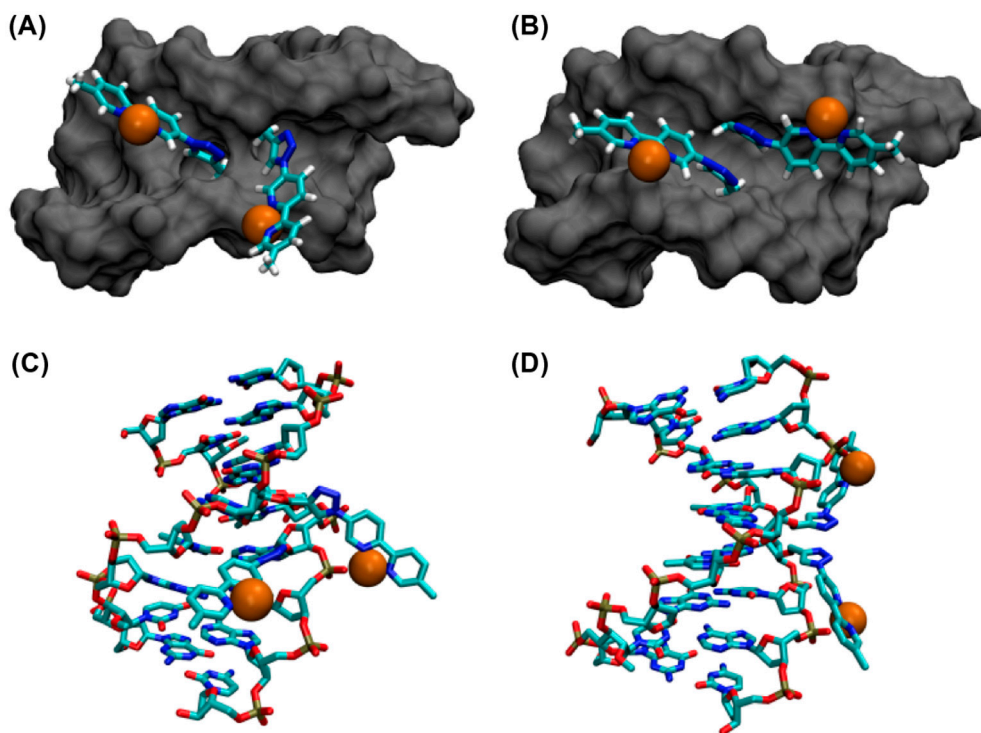
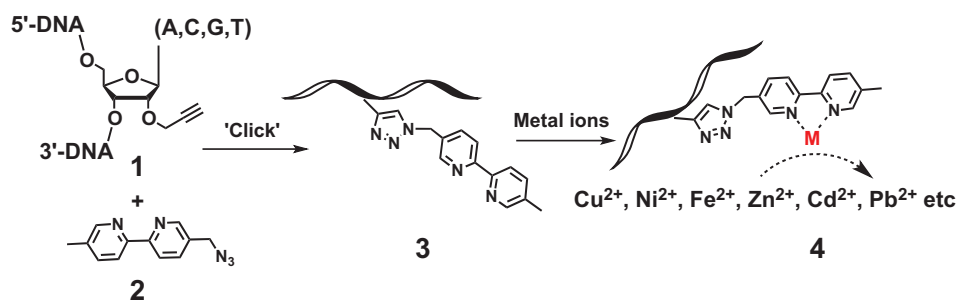
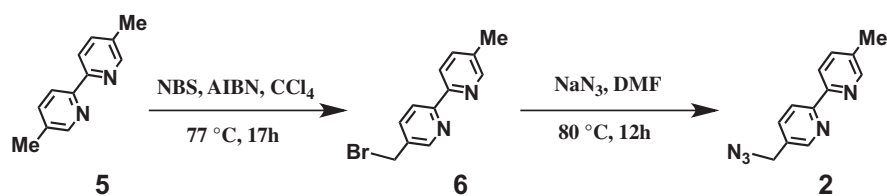


Figure 4. Computational models of bipyridine modified octamer DNA duplex [5'-G(2'-OMe-U)GT(2'-prop-A)CAC-3']<sub>2</sub> after 'click' reaction. (A,B) Surface view of the complex with the bipyridine rings extending cross and within the minor groove. (C,D) Stick view of the overall duplex structures with the two configurations of ligands and copper ions.



Scheme 1. Construction of metal-DNA complex by the site-specific incorporation of metal ions into DNA through a 'click' reaction between the propargyl modified DNA 1 and an azido modified bipyridine 2 as the metal chelating ligand.



Scheme 2. Synthesis of azido-bipyridine ligand 2 starting from 5,5'-dimethyl-bipyridine compound 5.

It is worthy to note that we performed the molecular dynamics simulations in 1 M NaCl solution. At such concentrations of salt, the copper ion is not expected to strongly coordinate with chloride ions (Jauniaux, Mawissa, Peellaerts, & Rodesch, 1992), which is what we observed in our simulations. Instead, we found that phosphate-bound copper ion coordinates with three water molecules, maintaining a six-membered coordination sphere (see Supplemental Figure S10).

### 3. Conclusion

In summary, we have described an efficient and facile method for constructing metallic DNA oligonucleotides through a 'Click' conjugation between 2'-propargyl-modified DNAs and a bipyridine metal chelating ligand. The bipyridine-modified DNA can serve as ideal structural scaffolds to bind different metal ions, which can be easily exchangeable in our DNA contexts. These complexes are thermally stable and do not cause major structural perturbations to the DNA duplex. In order to obtain structural insights, we solved the crystal structure of a propargyl modified DNA duplex and modeled two bipyridine ligands with two copper ions into the propargyl groups by molecular simulation. We observed potential interactions between coordinated copper and oxygen atoms in the DNA backbone. Such DNA-based metal chelating systems will be expected to have wide applications in the construction of artificial ribonucleases and chiral catalysis, as well as the delivery of metal ions.

## 4. Experimental

### 4.1. Materials and instruments

The organic reagents and solvents were purchased from Sigma-Aldrich and used directly without further purification. All solid reagents were dried under a high vacuum line prior to use. Air sensitive reactions were carried out under nitrogen. Analytical TLC plates pre-coated with silica gel F<sub>254</sub> (Dynamic Adsorbents) were used for monitoring reactions and visualized by UV light. Flash column chromatography was performed using silica gel (32–63  $\mu$ m). All <sup>1</sup>H, <sup>13</sup>C, and <sup>31</sup>P NMR spectra were recorded on a Bruker 400 spectrometer. Chemical shift values are in ppm. <sup>13</sup>C NMR signals were determined using APT technique. High-resolution MS data were achieved by ESI mass spectrometry at University at Albany, SUNY.

### 4.2. Synthesis of compound 6

To a stirred solution of 5,5'-dimethyl-2,2'-bipyridine, 5 (1.03 g, 5.60 mmol) and *N*-bromosuccinimide (1.02 g, 5.60 mmol) in anhydrous CCl<sub>4</sub> (50 mL) under argon at

ambient temperature was added catalytic AIBN (0.092 g, 0.56 mmol). The mixture was heated to reflux at 77°C for 17 h until the starting material was completely consumed. The mixture was filtered through silica gel when hot. The solution was cooled and filtered again to remove most of the di-bromo product. The filtrate was concentrated and purified by silica gel chromatography with 5% MeOH in CH<sub>2</sub>Cl<sub>2</sub> (contain 0.5% NEt<sub>3</sub>) to provide the product 0.59 g in 40% isolate yield. Rf 0.8, 5% MeOH in CH<sub>2</sub>Cl<sub>2</sub> (contain 0.5% NEt<sub>3</sub>). <sup>1</sup>H NMR (400 MHz, CDCl<sub>3</sub>):  $\delta$  8.68 (s, 1H), 8.62 (s, 1H), 8.37 (d, 1H, *J* = 8.2 Hz), 8.30 (d, *J* = 8.2 Hz, 1H), 7.85 (d, *J* = 8.2 Hz, 1H), 7.64 (d, *J* = 8.2 Hz, 1H), 4.55 (s, 2H), 2.41 (s, 3H). <sup>13</sup>C NMR (CDCl<sub>3</sub>, 100 MHz)  $\delta$  156.27, 153.07, 149.7, 137.44, 133.68, 120.7, 29.65, 25.14 ppm.

### 4.3. Synthesis of the azido-bipyridine compound 2

To a stirred solution of 5-(bromomethyl)-5'-methyl-2,2'-bipyridine, 6 (1.31 g, 5.0 mmol) in MeOH (25 mL) was added sodium azide (1.01 g, 15.39 mmol) and the mixture was heated to 70°C for overnight. When the starting material was completely consumed, the solvent was concentrated, diluted with CH<sub>2</sub>Cl<sub>2</sub> (20 mL) and the mixture was washed with brine, dried over sodium sulfate. The solvent was concentration and purified by silica gel chromatography using eluent 5% MeOH in CH<sub>2</sub>Cl<sub>2</sub> (with 1% NEt<sub>3</sub>) to give the product 1.06 g in 94% yield. Rf 0.4, 5% MeOH in CH<sub>2</sub>Cl<sub>2</sub> (with 1% NEt<sub>3</sub>). <sup>1</sup>H NMR (400 MHz, CDCl<sub>3</sub>)  $\delta$  8.63 (s, 1H), 8.53 (s, 1H), 8.43 (d, *J* = 8.2 Hz, 1H), 8.31 (d, *J* = 8.2 Hz, 1H), 7.80 (d, *J* = 8.2 Hz, 1H), 7.66 (d, *J* = 8.2 Hz, 1H), 4.45 (s, 2H), 2.42 (s, 3H). ESI-MS [M + H]<sup>+</sup> 226.111 (Calculated [M + H]<sup>+</sup>: 226.101) (Heck et al., 2002).

### 4.4. DNA oligonucleotide synthesis

The 2'-propargyl modified phosphoramidites were purchased from ChemGenes Corporation. All the DNA oligonucleotides were synthesized at 1.0- $\mu$ mol scales by solid phase synthesis using a MerMade MM8 synthesizer. All the phosphoramidites were dissolved in acetonitrile to a concentration of 0.07 M. 0.02 M I<sub>2</sub> in THF/Py/H<sub>2</sub>O solution was used as oxidizing reagent. All the other reagents are standard solutions obtained from ChemGenes or Glen Research. Synthesis was performed on the appropriate nucleoside immobilized via a succinate linker to control pore glass (CPG-500). All oligonucleotides were prepared in DMTr-on form. After synthesis, the oligos were cleaved from the solid support and fully deprotected with AMA (ammonium hydroxide: methylamine = 1:1) at 65°C for 30 min. The amines were removed by Speed-Vac concentrator before HPLC purification. After the DMTr-on purification, the detritylation was carried out by the treatment of 3%

trichloroacetic acid for 3 min, followed by the neutralization with triethylamine to pH 7.0. The DMTr-off oligonucleotides were purified again by HPLC.

#### 4.5. HPLC purification and analysis

The oligonucleotides were purified by reverse phase HPLC using a Zorbax SB-C18 column at a flow rate of 6 mL/min. Buffer A was 20 mM triethylammonium acetate, pH 7.1; buffer B contains 50% acetonitrile in 20 mM triethylammonium acetate, pH 7.1. A linear gradient from buffer A to 80% buffer B in 25 min was used to elute the oligos. The analysis was carried out using the same type of analytical column with the same eluent gradient. All the DNA oligos were analyzed by ESI-MS.

#### 4.6. DNA-click reaction

The propargyl modified DNA oligonucleotides (0.38 mM, 200  $\mu$ L in H<sub>2</sub>O) and azido-bipyridine compound 2 (10 mM, 114  $\mu$ L, H<sub>2</sub>O) were placed in a 1.5 mL vial. In a separate vial, 17  $\mu$ L CuBr solution (100 mM in DMSO/tBuOH 3:1) and 34  $\mu$ L CH<sub>3</sub>CN solution (100 mM in DMSO/tBuOH 3:1) were mixed and added to the DNA solution. The mixture was shaken at room temperature for overnight before being evaporated to near dryness in a Speed-Vac under 65°C. Sodium acetate (0.3 M, 100  $\mu$ L) was then added and the suspension was stirred for 1 h before 1 mL of ethanol was added. The vial was vortexed well and stored in a freezer (−80°C) for 1 h before centrifugation for 15 min at 13,000 rpm. The supernatant was carefully removed from the DNA pellet. Seventy per cent cold ethanol (−20°C) was used to wash the pellet for three times. Finally, the pellet was left drying on air and dissolved in water for HPLC purification.

#### 4.7. Mass spectrometric nucleic acid analysis

Samples were analyzed by direct infusion ESI on a ThermoFisher Scientific (Waltham, MA) Velos LTQ-OrbitrapVelos mass spectrometer. All analyses were performed in nanoflow mode using quartz emitters produced in house with a Sutter Instruments Co. (Novato, CA) P2000 laser pipette puller. Up to 5  $\mu$ L samples were typically loaded onto each emitter using a gel-loader pipette tip. A stainless steel wire was inserted in the back-end of the emitter to supply an ionizing voltage that ranged between 0.8 and 1.2 kV. Source temperature and desolvation conditions were adjusted by closely monitoring the incidence of ammonium adducts and water clusters. The instrument was calibrated using a mixture of 0.5 mg/ml of CsI in 50% methanol, which provided 1–3 ppm mass accuracy.

#### 4.8. UV-melting temperature $T_m$ study

Solutions of the duplex DNAs (0.5  $\mu$ M) were prepared by dissolving the purified DNAs in sodium phosphate (10 mM, pH 6.5) buffer containing 100 mM NaCl. The solutions were heated to 85°C for 3 min, then cooled down slowly to room temperature, and stored at 4°C for 2 h before  $T_m$  measurement. Thermal denaturation was performed in a Cary 300 UV–Visible Spectrophotometer with a temperature controller. The temperature reported is the block temperature. Each denaturing curves were acquired at 260 nm by heating and cooling from 5 to 80°C for four times in a rate of 0.5°C/min. All the melting curves were repeated for at least four times.

#### 4.9. Crystallization and diffraction data collection

DNA samples (0.5 mM duplex) were heated to 80°C for 3 min, cooled slowly to room temperature, and placed at 4°C overnight before crystallization. Nucleic Acid Mini Screen and Natrix Kits (Hampton Research) were used to screen crystallization conditions at different temperatures using the hanging-drop vapor diffusion method. Perfluoropolyether was used as cryoprotectant for the crystal mounting. Data were collected under a liquid nitrogen stream at −174°C. The diffraction data were collected at beam lines ALS 8.2.2 in Lawrence Berkeley National Laboratory. Data were collected at a wavelength of 1.0 Å. Crystals were exposed for 1 s per image with a 1 degree oscillation angle. All data were processed using HKL2000 and DENZO/ SCALEPACK (Otwinowski & Minor, 1997).

#### 4.10. Structure determination and refinement

The 2'-propargyl modified DNA structure presented here was solved by molecular replacement with PHASER using PDB structure 1Z7I as the search model, followed by the refinement using Refmac. The usual refinement protocol includes positional refinement, restrained B-factor refinement, and bulk solvent correction. The stereochemical topology and geometrical restraint parameters of DNA/RNA were applied (Parkinson, Vojtechovsky, Clowney, Brünger, & Berman, 1996). After several cycles of refinement, a number of highly ordered waters were added. Cross-validation (Brünger et al., 1998) with a 5% test set was monitored during the refinement. The  $\sigma_A$ -weighted maps (Read, 1986) of the  $(2m|Fo| - D|Fc|)$  and the difference  $(m|Fo| - D|Fc|)$  density maps were computed and used to build the 2'-propargyl group.

#### 4.11. Molecular simulation study

We performed extensive MD simulations of the DNA duplex with and without the modifications totalling over

a microsecond of simulation data. The crystal structure of DNA duplex with two 2'-propargyl groups was used as the template to which the two bipyridine ligands with copper ions are added. The ligands (one per strand) was constructed in an 'open' type conformation, i.e. pointing away from the duplex. We attached copper ions to the ligands imparting a +2 charge, followed by MD simulations to predict the structural preferences of the ligand with respect to the rest of the duplex. Molecular dynamics simulations were performed using Gromacs-4.6.3 (Hess, Kutzner, van der Spoel, & Lindahl, 2008). The simulation system included the DNA duplex with/without ligands in a solution of 1 M NaCl solution in a 3D periodic box. The box size was  $5 \times 5 \times 5 \text{ nm}^3$  containing 85  $\text{Na}^+$  ions, 75  $\text{Cl}^-$  ions and 3769 water molecules. The systems were subjected to energy minimization to prevent any overlap of atoms, followed by a 10 ns equilibration run. Configurations were chosen at 2 ns intervals from the equilibration run, for five independent 100 ns production runs, totalling 0.5 microsecond of trajectory for analysis. The MD simulations incorporated leapfrog algorithm with a 2 fs time step to integrate the equations of motion. The system was maintained at 300 K using the velocity rescaling thermostat (Bussi, Donadio, & Parrinello, 2007). The long-ranged electrostatic interactions were calculated using particle mesh Ewald (PME) (Darden, York, & Pedersen, 1993) algorithm with a real space cut-off of 1.2 nm. LJ interactions were also truncated at 1.2 nm. TIP3P model (Jorgensen, Chandrasekhar, Madura, Impey, & Klein, 1983) was used represent the water molecules, and LINCS algorithm was used to constrain the motion of hydrogen atoms bonded to heavy atoms. Coordinates of the DNA molecule were stored every 10 ps for further analysis.

PARMBSC1 forcefield (Ivani et al., 2016), with modified backbone, glycosidic and sugar torsions was used for the DNA simulations. AMBER-type (Wang, Wolf, Caldwell, Kollman, & Case, 2004) force field parameters were generated for the propargyl group as follows. For obtaining the partial charges on the atoms, we used the online RESP charge-fitting server, RED (Dupradeau et al., 2010). The geometry of the modified nucleoside was energy minimized, and Hartree-Fock level theory and 6-31G\* basis sets were employed to arrive at a set of partial charges (Cornell, Cieplak, Bayly, & Kollmann, 1993). The parameters for the propargyl modified nucleoside and the bipyridine ligands were listed in the end of the supporting information.

### Supplementary material

The supplementary material for this article is available online at <https://doi.org/10.1080/07391102.2018.1441071>.

### Acknowledgments

The X-ray diffraction data were collected at the Advanced Light Source (ALS) beamlines 8.2.2.

### Disclosure statement

No potential conflict of interest was reported by the authors.

### Funding

This work was supported by the start-up fund from University at Albany, SUNY. The Berkeley Center for Structural Biology is supported in part by the National Institutes of Health, National Institute of General Medical Sciences, and the Howard Hughes Medical Institute. The Advanced Light Source is supported by the Director, Office of Science, Office of Basic Energy Sciences, of the US Department of Energy [contract number DE-AC02-05CH11231] and the authors also thank the Key Research and Development Project of China (2016YFA0500600) for the financial support.

### References

- Berndl, S., Herzig, N., Kele, P., Lachmann, D., Li, X., Wolfbeis, O. S., & Wagenknecht, H. A. (2009). Comparison of a nucleosidic vs non-nucleosidic postsynthetic 'click' modification of DNA with base-labile fluorescent probes. *Bioconjugate Chemistry*, 20, 558–564.
- Bos, J., & Roelfes, G. (2014). Artificial metalloenzymes for enantioselective catalysis. *Current Opinion in Chemical Biology*, 19, 135–143.
- Brünger, A. T., Adams, P. D., Clore, G. M., DeLano, W. L., Gros, P., Grosse-Kunstleve, R. W., ... Warren, G. L. (1998). Crystallography & NMR system: A new software suite for macromolecular structure determination. *Acta Crystallographica Section D Biological Crystallography*, 54, 905–921.
- Bussi, G., Donadio, D., & Parrinello, M. (2007). Canonical sampling through velocity rescaling. *The Journal of Chemical Physics*, 126, 014101.
- Chen, Y. J., Groves, B., Muscat, R. A., & Seelig, G. (2015). DNA nanotechnology from the test tube to the cell. *Nature Nanotechnology*, 10, 748–760.
- Cornell, W. D., Cieplak, P., Bayly, C. I., & Kollmann, P. A. (1993). Application of RESP charges to calculate conformational energies, hydrogen bond energies, and free energies of solvation. *Journal of the American Chemical Society*, 115, 9620–9631.
- Cutler, J. I., Auyeung, E., & Mirkin, C. A. (2012). Spherical nucleic acids. *Journal of the American Chemical Society*, 134, 1376–1391.
- Darden, T., York, D., & Pedersen, L. (1993). Particle mesh Ewald: An  $N \cdot \log(N)$  method for Ewald sums in large systems. *The Journal of Chemical Physics*, 98, 10089–10092.
- Deng, Z., Samanta, A., Nangreave, J., Yan, H., & Liu, Y. (2012). Robust DNA-functionalized core/shell quantum dots with fluorescent emission spanning from UV-vis to near-IR and compatible with DNA-directed self-assembly. *Journal of the American Chemical Society*, 134, 17424–17427.
- Dey, S., & Jäschke, A. (2015). Tuning the stereoselectivity of a DNA-catalyzed michael addition through covalent modification. *Angewandte Chemie International Edition*, 54, 11279–11282.

- Douglas, S. M., Dietz, H., Liedl, T., Högberg, B., Graf, F., & Shih, W. M. (2009). Self-assembly of DNA into nanoscale three-dimensional shapes. *Nature*, *459*, 414–418.
- Douglas, S. M., Marblestone, A. H., Teerapittayanon, S., Vazquez, A., Church, G. M., & Shih, W. M. (2009). Rapid prototyping of 3D DNA-origami shapes with caDNAno. *Nucleic Acids Research*, *37*, 5001–5006.
- Dupradeau, F. Y., Pigache, A., Zaffran, T., Savineau, C., Lelong, R., Grivel, N., ... Cieplak, P. (2010). The R.E.D. tools: Advances in RESP and ESP charge derivation and force field library building. *Physical Chemistry Chemical Physics*, *12*, 7821–7839.
- Duprey, J. L., Takezawa, Y., & Shionoya, M. (2013). Metal-locked DNA three-way junction. *Angewandte Chemie International Edition*, *52*, 1212–1216.
- Ellington, A. D., & Szostak, J. W. (1990). In vitro selection of RNA molecules that bind specific ligands. *Nature*, *346*, 818–822.
- Fink, H. W., & Schönenberger, C. (1999). Electrical conduction through DNA molecules. *Nature*, *398*, 407–410.
- Garg, T., Rath, G., & Goyal, A. K. (2015). Biomaterials-based nanofiber scaffold: Targeted and controlled carrier for cell and drug delivery. *Journal of Drug Targeting*, *23*, 202–221.
- Garg, T., Singh, O., Arora, S., & Murthy, R. (2012). Scaffold: A novel carrier for cell and drug delivery. *Critical Reviews in Therapeutic Drug Carrier Systems*, *29*, 1–63.
- Gierlich, J., Burley, G. A., Gramlich, P. M., Hammond, D. M., & Carell, T. (2006). Click chemistry as a reliable method for the high-density postsynthetic functionalization of alkyne-modified DNA. *Organic Letters*, *8*, 3639–3642.
- Gjonaj, L., & Roelfes, G. (2013). Novel catalyst design by using cisplatin to covalently anchor catalytically active copper complexes to DNA. *ChemCatChem*, *5*, 1718–1721.
- Grötl, M., Douglas, M., Eritja, R., & Sproat, B. S. (1998). 2'-O-Propargyl oligoribonucleotides: Synthesis and hybridisation. *Tetrahedron*, *54*, 5899–5914.
- Gupta, M., Tiwari, S., & Vyas, S. (2012). Structuring polymers for delivery of DNA-based therapeutics: Updated insights. *Critical Reviews in Therapeutic Drug Carrier Systems*, *29*, 447–485.
- Hall, J., Husken, D., & Haner, R. (1996). Towards artificial ribonucleases: The sequence-specific cleavage of RNA in a duplex. *Nucleic Acids Research*, *24*, 3522–3526.
- Heck, R., Dumarcay, F., & Marsura, A. (2002). New scaffolds for supramolecular chemistry: Upper-rim fully tethered 5-methyleneureido-5'-methyl-2,2'-bipyridyl cyclodextrins. *Chemistry-A European Journal*, *8*, 2438–2445.
- Hess, B., Kutzner, C., van der Spoel, D., & Lindahl, E. (2008). GROMACS 4: Algorithms for highly efficient, load-balanced, and scalable molecular simulation. *Journal of Chemical Theory and Computation*, *4*, 435–447.
- Holzhauser, C., Rubner, M. M., & Wagenknecht, H. A. (2013). Energy-transfer-based wavelength-shifting DNA probes with 'clickable' cyanine dyes. *Photochemical & Photobiological Sciences*, *12*, 722–724.
- Hong, B. J., Eryazici, I., Bleher, R., Thaner, R. V., Mirkin, C. A., & Nguyen, S. T. (2015). Directed assembly of nucleic acid-based polymeric nanoparticles from molecular tetravalent cores. *Journal of the American Chemical Society*, *137*, 8184–8191.
- Ipe, B. I., Yoosaf, K., & Thomas, K. G. (2006). Functionalized gold nanoparticles as phosphorescent nanomaterials and sensors. *Journal of the American Chemical Society*, *128*, 1907–1913.
- Ivani, I., Dans, P. D., Noy, A., Pérez, A., Faustino, I., Hospital, A., ... Orozco, M. (2016). Parmbsc1: A refined force field for DNA simulations. *Nature Methods*, *13*, 55–58.
- Jauniaux, E., Mawissa, C., Peellaerts, C., & Rodesch, F. (1992). Nuchal cord in normal third-trimester pregnancy: A color Doppler imaging study. *Ultrasound in Obstetrics & Gynecology*, *2*, 417–419.
- Jiang, J., Sheng, J., Carrasco, N., & Huang, Z. (2007). Selenium derivatization of nucleic acids for crystallography. *Nucleic Acids Research*, *35*, 477–485.
- Jorgensen, W. L., Chandrasekhar, J., Madura, J. D., Impey, R. W., & Klein, M. L. (1983). Comparison of simple potential functions for simulating liquid water. *The Journal of Chemical Physics*, *79*, 926–935.
- Klotsa, D., Römer, R. A., & Turner, M. S. (2005). Electronic transport in DNA. *Biophysical Journal*, *89*, 2187–2198.
- Kuzyk, A., Schreiber, R., Fan, Z., Pardatscher, G., Roller, E. M., Högele, A., ... Liedl, T. (2012). DNA-based self-assembly of chiral plasmonic nanostructures with tailored optical response. *Nature*, *483*, 311–314.
- Liu, X., Diao, H., & Nishi, N. (2008). Applied chemistry of natural DNA. *Chemical Society Reviews*, *37*, 2745–2757.
- Macfarlane, R. J., O'Brien, M. N., Petrosko, S. H., & Mirkin, C. A. (2013). Nucleic acid-modified nanostructures as programmable atom equivalents: Forging a new 'table of elements'. *Angewandte Chemie International Edition*, *52*, 5688–5698.
- Maune, H. T., Han, S. P., Barish, R. D., Bockrath, M., Goddard III, W. A., Rothmund, P. W., & Winfree, E. (2010). Self-assembly of carbon nanotubes into two-dimensional geometries using DNA origami templates. *Nature Nanotechnology*, *5*, 61–66.
- McLaughlin, C. K., Hamblin, G. D., & Sleiman, H. F. (2011). Supramolecular DNA assembly. *Chemical Society Reviews*, *40*, 5647–5656.
- Oltra, N. S., & Roelfes, G. (2008). Modular assembly of novel DNA-based catalysts. *Chemical Communications*, 6039–6041.
- Otwinowski, Z., & Minor, W. (1997). Processing of X-ray diffraction data collected in oscillation mode. *Methods in Enzymology*, *276*, 307–326.
- Park, S., Zheng, L., Kumakiri, S., Sakashita, S., Otomo, H., Ikehata, K., & Sugiyama, H. (2014). Development of DNA-based hybrid catalysts through direct ligand incorporation: Toward understanding of DNA-based asymmetric catalysis. *ACS Catalysis*, *4*, 4070–4073.
- Parkinson, G., Vojtechovsky, J., Clowney, L., Brünger, A. T., & Berman, H. M. (1996). New parameters for the refinement of nucleic acid-containing structures. *Acta Crystallographica Section D Biological Crystallography*, *52*, 57–64.
- Pujari, S. S., Leonard, P., & Seela, F. (2014). Oligonucleotides with 'clickable' sugar residues: Synthesis, duplex stability, and terminal versus central interstrand cross-linking of 2'-O-propargylated 2-aminoadenosine with a bifunctional azide. *The Journal of Organic Chemistry*, *79*, 4423–4437.
- Read, R. J. (1986). Improved Fourier coefficients for maps using phases from partial structures with errors. *Acta Crystallographica Section A*, *42*, 140–149.
- Richters, T., Krug, O., Kösters, J., Hepp, A., & Müller, J. (2014). A family of 'click' nucleosides for metal-mediated base pairing: Unravelling the principles of highly stabilizing metal-mediated base pairs. *Chemistry-A European Journal*, *20*, 7811–7818.

- Rioz-Martínez, A., & Roelfes, G. (2015). DNA-based hybrid catalysis. *Current Opinion in Chemical Biology*, 25, 80–87.
- Robertson, D. L., & Joyce, G. F. (1990). Selection *in vitro* of an RNA enzyme that specifically cleaves single-stranded DNA. *Nature*, 344, 467–468.
- Roche, S. (2003). Sequence dependent DNA-mediated conduction. *Physical Review Letters*, 91, 22.
- Rothemund, P. W. (2006). Folding DNA to create nanoscale shapes and patterns. *Nature*, 440, 297–302.
- Sakamoto, S., Tamura, T., Furukawa, T., Komatsu, Y., Ohtsuka, E., Kitamura, M., & Inoue, H. (2003). Highly efficient catalytic RNA cleavage by the cooperative action of two Cu(II) complexes embodied within an antisense oligonucleotide. *Nucleic Acids Research*, 31, 1416–1425.
- Scharf, P., & Müller, J. (2013). Nucleic acids with metal-mediated base pairs and their applications. *ChemPlusChem*, 78, 20–34.
- Seeman, N. C. (1982). Nucleic acid junctions and lattices. *Journal of Theoretical Biology*, 99, 237–247.
- Seeman, N. C. (2010). Nanomaterials based on DNA. *Annual Review of Biochemistry*, 79, 65–87.
- Sheng, J., Jiang, J., Salon, J., & Huang, Z. (2007). Synthesis of a 2'-Se-thymidine phosphoramidite and its incorporation into oligonucleotides for crystal structure study. *Organic Letters*, 9, 749–752.
- Stubinitzky, C., Bijeljanin, A., Antusch, L., Ebeling, D., Hölscher, H., & Wagenknecht, H. A. (2014). Bifunctional DNA architectonics: Three-way junctions with sticky perylene bisimide caps and a central metal lock. *Chemistry-A European Journal*, 20, 12009–12014.
- Takezawa, Y., & Shionoya, M. (2012). Metal-mediated DNA base pairing: Alternatives to hydrogen-bonded Watson–Crick base pairs. *Accounts of Chemical Research*, 45, 2066–2076.
- Thaner, R. V., Eryazici, I., Farha, O. K., Mirkin, C. A., & Nguyen, S. T. (2014). Facile one-step solid-phase synthesis of multitopic organic-DNA hybrids via 'click' chemistry. *Chemical Science*, 5, 1091–1096.
- Tuerk, C., & Gold, L. (1990). Systematic evolution of ligands by exponential enrichment: RNA ligands to bacteriophage T4 DNA polymerase. *Science*, 249, 505–510.
- Wang, K., Huang, J., Yang, X., He, X., & Liu, J. (2013). Recent advances in fluorescent nucleic acid probes for living cell studies. *The Analyst*, 138, 62–71.
- Wang, J., Wolf, R. M., Caldwell, J. W., Kollman, P. A., & Case, D. A. (2004). Development and testing of a general amber force field. *Journal of Computational Chemistry*, 25, 1157–1174.
- Williams, A., Staroseletz, Y., Zenkova, M. A., Jeannin, L., Aojula, H., & Bichenkova, E. V. (2015). Peptidyl-oligonucleotide conjugates demonstrate efficient cleavage of RNA in a sequence-specific manner. *Bioconjugate Chemistry*, 26, 1129–1143.
- Xu, H., Li, Q., Wang, L., He, Y., Shi, J., Tang, B., & Fan, C. (2014). Nanoscale optical probes for cellular imaging. *Chemical Society Reviews*, 43, 2650–2661.
- Yamada, T., Peng, C. G., Matsuda, S., Addepalli, H., Jayaprakash, K. N., Alam, M. R., ... Rajeev, K. G. (2011). Versatile site-specific conjugation of small molecules to siRNA using click chemistry. *The Journal of Organic Chemistry*, 76, 1198–1211.